A STUDY OF VERTICAL GROUND MOTION SHOWING THE FREE SURFACE EFFECT

A thesis submitted in partial fulfillment
of the requirements for the degree of
Master of Science in Geophysics at
New Mexico Institute of Mining
and Technology.

by
Norman E. Biles

June 1967

ACKNOWLEDGMENTS

The following study was made under the direction of Dr. Allan R. Sanford of the New Mexico Institute of Mining and Technology. The author wishes to express his appreciation to Dr. Sanford for suggestion of the thesis topic and his helpful assistance and guidance during the preparation of the thesis.

I also wish to thank the members of my thesis committee for their help in the final preparation of this thesis.

My thanks go to Mr. Roy A. McCrory for the use of his computer program for calculating power spectra.

TABLE OF CONTENTS

	Page
ABSTRACT	vii
INTRODUCTION	1
INSTRUMENTATION	8
LOCATION	8
INSTRUMENTS	11
DATA	14
SOURCES	14
Microearthquakes	14
Man Made Seismic Events	19
ACQUIRING DATA	19
TREATMENT OF RECORDS	20
PRESENTATION AND DISCUSSION OF DATA	22
AMPLITUDE AND FREQUENCY RELATIONSHIPS	22
AMPLITUDE AND OVERBURDEN RELATIONSHIPS	31
FREQUENCY FILTERING	40
CONCLUSIONS AND SUGGESTIONS FOR FURTHER STUDY	45
REFERENCES	48

LIST OF FIGURES

Figure		Page
1.	Graphs of the ratio of horizontal and vertical displacements to the incident amplitude at a free surface for different values of Poisson's ratio.	4
2.	Map showing location of tunnel in Socorro Mountain.	9
3.	Cross-section of mine tunnel showing instrument pad locations.	10
4.	Trace of a microearthquake recorded at the surface.	15
5.	Plot of S motion frequency against first motion frequency.	17
6.	Power spectral density of the P and S arrivals of a microearthquake recorded at the free surface.	18
7.	Two microearthquakes showing amplitude doubling in their first motions.	23
8.	Four different traces of one microearthquake showing the effect of overburden thickness on trace amplitudes.	24
9.	Ratio of amplitudes of first motions at station C to station F versus first motion frequency.	26
10.	Ratio of amplitudes of first motions at station C to station G versus first motion frequency.	26
11.	Ratio of amplitudes of first motions at station C to station F versus first motion wavelength.	28
12.	Ratio of amplitudes of S motions at station C to station F versus S motion frequency.	29
13.	Ratio of amplitudes of S motions at station C to station F versus first P motion frequency.	29
14.	Relative first P motion amplitudes versus overburden for frequencies from 21 to 31 cps.	32

Figure		Page
15.	Relative first P motion amplitudes versus overburden for frequencies from 15 to 20 cps.	32
16.	Relative first P motion amplitudes versus overburden for frequencies from 6 to 9 cps.	33
17.	Relative S motion amplitudes versus overburden for S motion frequencies from 6 to 12 cps.	35
18.	Relative S motion amplitudes versus overburden for S motion frequencies from 13 to 16 cps.	35
19.	Three traces of one microearthquake showing S phase amplitude increase at station G relative to station F.	36
20.	Four different traces of one microearthquake showing effect of overburden thickness on amplitude.	37
21.	Two traces of a microearthquake showing the effect of low frequency on the amplitude of the first motion.	38
22.	Power spectrum of a microearthquake trace (Aug. 4, 1966) at station C (free surface).	41
23.	Power spectrum of a microearthquake trace (Aug. 4, 1966) at station E (48 feet overburden).	42
24.	Power spectrum of a microearthquake trace (Aug. 4, 1966) at station G (134 feet overburden).	43

ABSTRACT

Amplitudes of vertical ground velocity were recorded on the free surface and at different depths beneath the surface. Microearthquakes and man-made explosions were the principle sources of elastic waves which produced ground motion. Ground motion detectors (seismometers) were placed in a mine tunnel on the eastern slope of Socorro Mountain. One instrument remained outside the entrance for measuring motion at the free surface and the others were distributed along the tunnel at different depths beneath the surface. Data was taken on high-speed strip-chart recorders at 25 mm/sec. Magnification of ground motion was 0.8 million at a frequency of 20 cps.

The amplitude and frequency of the first half-cycle of the P phase and the maximum S phase motion on the seismograms were used for comparing amplitudes of ground motion at the surface to ground motion below the surface. The ratios of amplitudes on the free surface to amplitudes at depth were found to depend on the frequency of the motion and depth beneath the surface. For frequencies of 15 to 31 cps, the maximum amplitude change for the initial P motion occurred in the first 50 feet beneath the surface. For frequencies higher than 15 cps, the free surface motion of the first P arrival was twice the amplitude of ground motion recorded at depths greater than 50 feet. S motion amplitudes also decreased with depth from the free surface but did not reach

the maximum expected amplitude reduction at the deepest recording station (134 feet overburden).

The seismometer location seemed to have an influence on whether or not there were high frequencies in the seismogram.

A STUDY OF VERTICAL GROUND MOTION SHOWING THE FREE SURFACE EFFECT

INTRODUCTION

The amplitude and character of a seismogram is influenced by the seismometer's location. A seismometer on the surface should measure motion of different amplitude and character than an identical instrument located beneath the surface. This study is intended to show that first motion trace amplitudes of a seismogram recorded on the surface are actually twice the corresponding trace amplitudes recorded beneath the surface. The minimum depths beneath the surface at which the amplitude is halved and the influence of frequency on amplitude at these depths were of particular interest.

Differences in amplitude and character of the seismogram were found experimentally by recording microearthquakes with sharp or recognizable first motions at four locations on high-gain high-speed seismographs. The transducer for one instrument was placed on the free surface, the others below ground at depths to 134 feet. The geometry of the instrument location was such that all four transducers were at essentially the same distance from the source. Microearthquakes were the principle source of data. Nearby

surface explosions also produced usable records for comparing amplitudes of ground motion at different locations. First motion amplitudes and peak to peak S motion amplitudes were measured directly from the seismograms. The data is presented in graphical form with examples of seismograms to show effects of overburden on character and frequency content of the trace.

The study of ground motion at the surface involves the reflection of elastic waves at a free surface (the earth-air interface). It is assumed that the earth-air interface is a good approximation to the ideal (solid-vacuum) interface.

An incident P or SV wave will generate both P and SV reflections at a free surface. There are no transmitted phases and the incident energy is conserved and partitioned between the two reflected phases. During the reflection process for an incident P wave the free surface offers essentially no resistance to normal stresses. The surface is unrestrained and moves under the forward motion of the incident wave. At the surface the displacements of rock particles representing the incident and reflected pulse add to produce twice the amplitude of the incident wave (Dix, 1952). The incident and reflected P (or SV) waves are 180 degrees out of phase when reflected at a free surface. Doubling or near doubling also occurs for incident SV waves at the free surface. In either case the angle of incidence should be small if doubling is to take place.

The effect of the free surface on ground motion has been predicted theoretically. The problem of displacements at a solid-vacuum interface is a special case of elastic waves impinging on the boundary between two solids having different elastic properties. The theory for predicting amplitude ratios of ground motion at a solid-solid boundary can be found from any of the following: (1) the Zoeppritz equations (Richter, 1958), (2) the Knott equations (Macelwane, 1932), or (3) the solution to a boundary value problem using potential functions and the equations of motion (Ewing, Jardetsky, and Press, 1957). The theory specifies that the rock should be homogeneous and isotropic and that the incident wave should be a steady-state sinusoidal elastic wave. These conditions also apply for reflection at a free surface. The absence of transmitted phases and the fact that normal and shearing stresses are zero at a free surface boundary simplify the use of the above equations.

Numerical calculations giving the ratios of the amplitudes of displacement at the free surface (u and w) to the amplitude of the incident wave have been published most completely in two papers (Gutenberg, 1944; Knopoff, et al., 1957). Gutenberg's curves for both incident P and SV waves are shown in Figure 1. The curves presented by Knopoff (1957) cover a much wider range of Poisson's ratios. Poisson's ratio is a function of the type of material and will significantly effect amplitude ratios at large angles of incidence.

Gutenberg's graphs present ratios of free surface displacements to incident amplitudes for different angles of

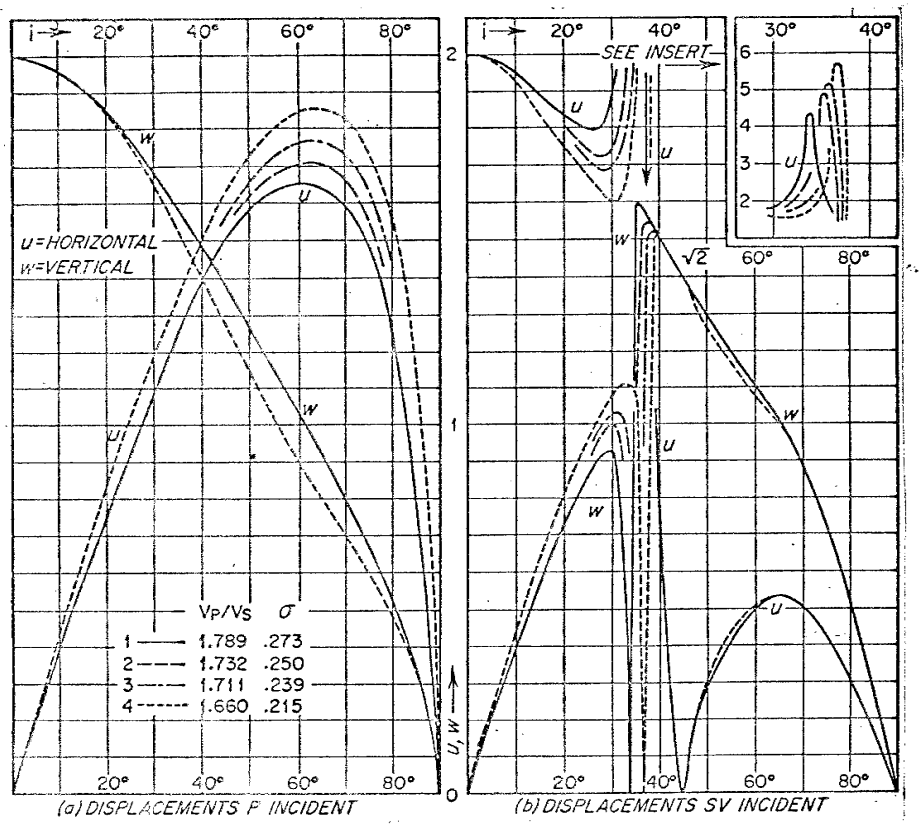

Figure 1. Graphs of the ratio of horizontal and vertical displacements to the incident amplitude at a free surface for different values of Poisson's ratio. (After Gutenberg, 1944)

incidence. This study was based on ratios of the trace amplitudes of vertical component seismograms. All ratios were with respect to the trace amplitudes for the seismograms obtained at the free surface. Theoretical amplitude ratios comparable to those used in this study can be found from Gutenberg's graphs. The vertical component of the incident wave at the free surface is found for a specific angle of incidence from Gutenberg's curves and then compared to the vertical component of motion for an incident wave with an amplitude of one. By changing the angle of incidence one can show that doubling occurs at the surface for the vertical component of incident P waves for angles of incidence less than 30 degrees. Similar computations for the vertical component of the SV waves show that the ratio is slightly greater than two for angles of incidence less than 30 degrees.

Agreement between theory and experimental results depends on how well the specified theoretical conditions are fulfilled. A finite wave train with a definite beginning followed by a series of P and S wave arrivals is not a steady-state elastic wave. It was of interest to see whether the first motion on a seismogram would show amplitude doubling even though it is not steady-state motion. The S phase portion of the seismogram was also used to compare ground motion at the surface to ground motion beneath the surface.

Previous experimental research on free surface motion has been confined to observations of horizontal ground

motions (Kanai and Tanaka, 1951; Kanai et al., 1959) with the exception of a paper by Tatel and Tuve (1958). Kanai and Tanaka (1951) compared horizontal components of ground motion produced by earthquakes at depths to 450 meters with the corresponding surface motion. Ratios of the amplitudes of initial P motion between zero and 450 meters depth ranged from 1.0 to 2.0. Ratios of the amplitudes of initial S motion ranged from 1.1 to 1.9. Epicenters at sea gave higher ratios (1.5 to 2.0) than land epicenters (1.0 to 1.5) which they attributed to a smaller angle of incidence for shocks located beneath the sea. The second paper by Kanai (1959) again analyzes horizontal components of seismic waves using a power spectral analysis of the seismograms. The emphasis was on multiple reflections in a superficial surface layer which might produce a resonant effect and give large amplitude ratios between recorded motion at the surface and underground. Current research in Japan on ground motion at different depths deals primarily with this resonant effect (Shima, 1962).

Tatel and Tuve (1958) investigated vertical ground motion due to body waves from a man-made source at 3000 feet below the surface. Seismometers were placed in wells two to three kilometers away from the shot and at the same depth as the shot. They observed a five-fold amplitude increase in the first arrival for a seismometer on the surface compared with a seismometer at a depth of 3000 feet. Reasons they proposed for the observed amplitude difference were: (1) the buried seismometer measured only vertical motion and the energy from the

shot was likely to produce predominantly horizontal motion, (2) free surface doubling increased the surface motion, and (3) velocity gradients might have increased the surface motion. They also observed a similarity in the two seismograms but commented that a surface seismogram would be more complex due to wave conversion and scattering at the surface.

INSTRUMENTATION

LOCATION

The site of the experiments was two miles west of the Research Building on the New Mexico Institute of Mining and Technology campus (Figure 2). An abandoned mine tunnel (line AB in Figure 2) provided means for placing seismometers at different depths beneath the surface. Figure 3 shows a cross-section of the mine tunnel. Cement pads were established along the floor of the tunnel and at the entrance of the tunnel. These served as level platforms for the seismometers.

Station locations were as follows: (1) station C, at the tunnel entrance and on the free surface, (2) station D, 25 feet inside the tunnel and 20 feet beneath the surface, (3) station E, 100 feet inside the tunnel and 48 feet beneath the surface, (4) station F, 200 feet inside the tunnel and 89 feet beneath the surface, and (5) station G, 300 feet inside the tunnel and 134 feet beneath the surface. All depths beneath the surface are measured vertically from the station location to the surface.

The tunnel is located in Tertiary volcanic rock (Smith, 1963). The rock is of uniform composition and essentially homogeneous along the length of the tunnel. The P wave velocity in the tunnel rock is in the neighborhood of 10,000 ft/sec (Personal communication, Sanford). This velocity is based on a seismic time-distance plot made a few years ago. The poor quality of the seismic records prevented a detailed velocity profile along the tunnel.

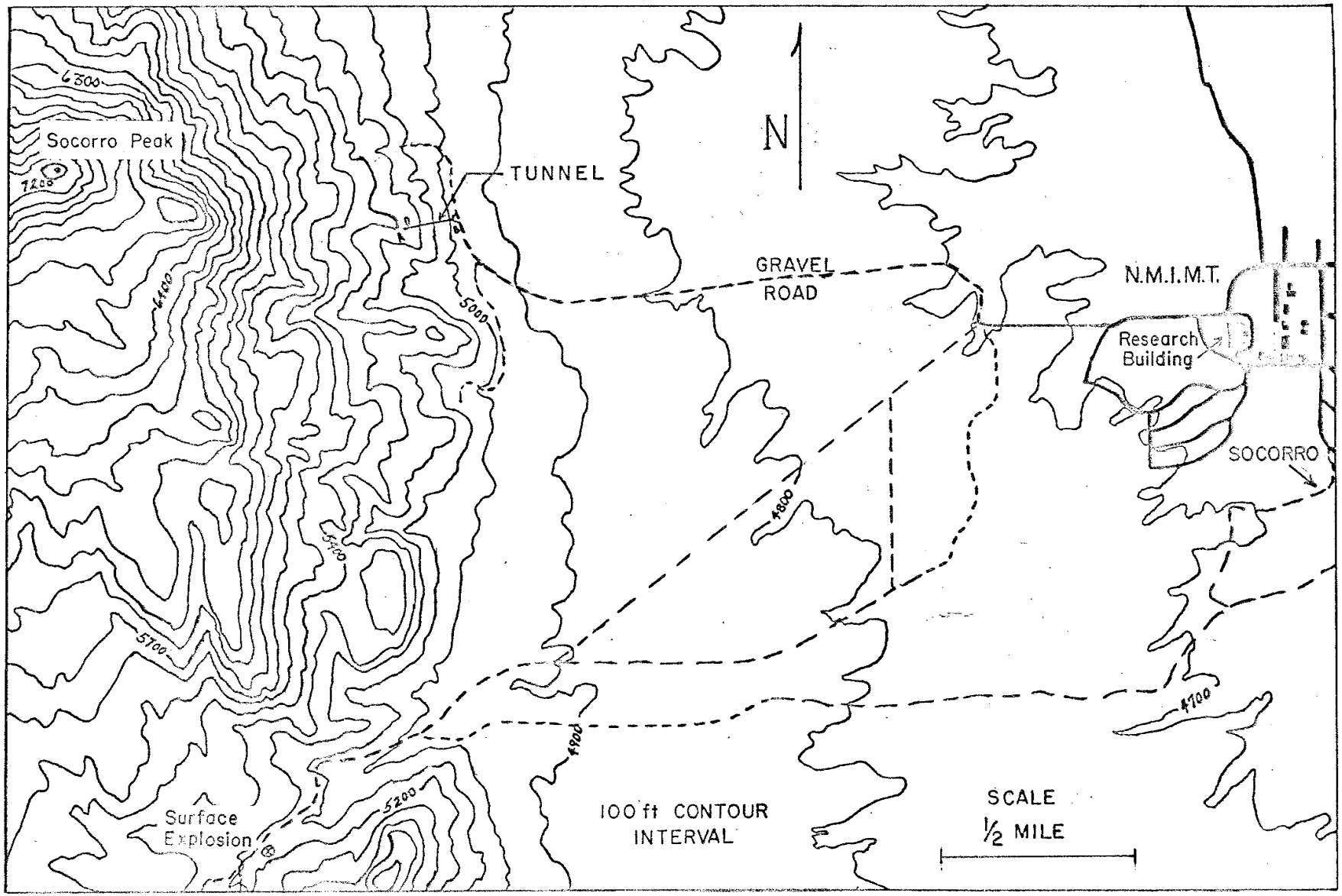

Figure 2. Map showing location of tunnel in Socorro Mountain.

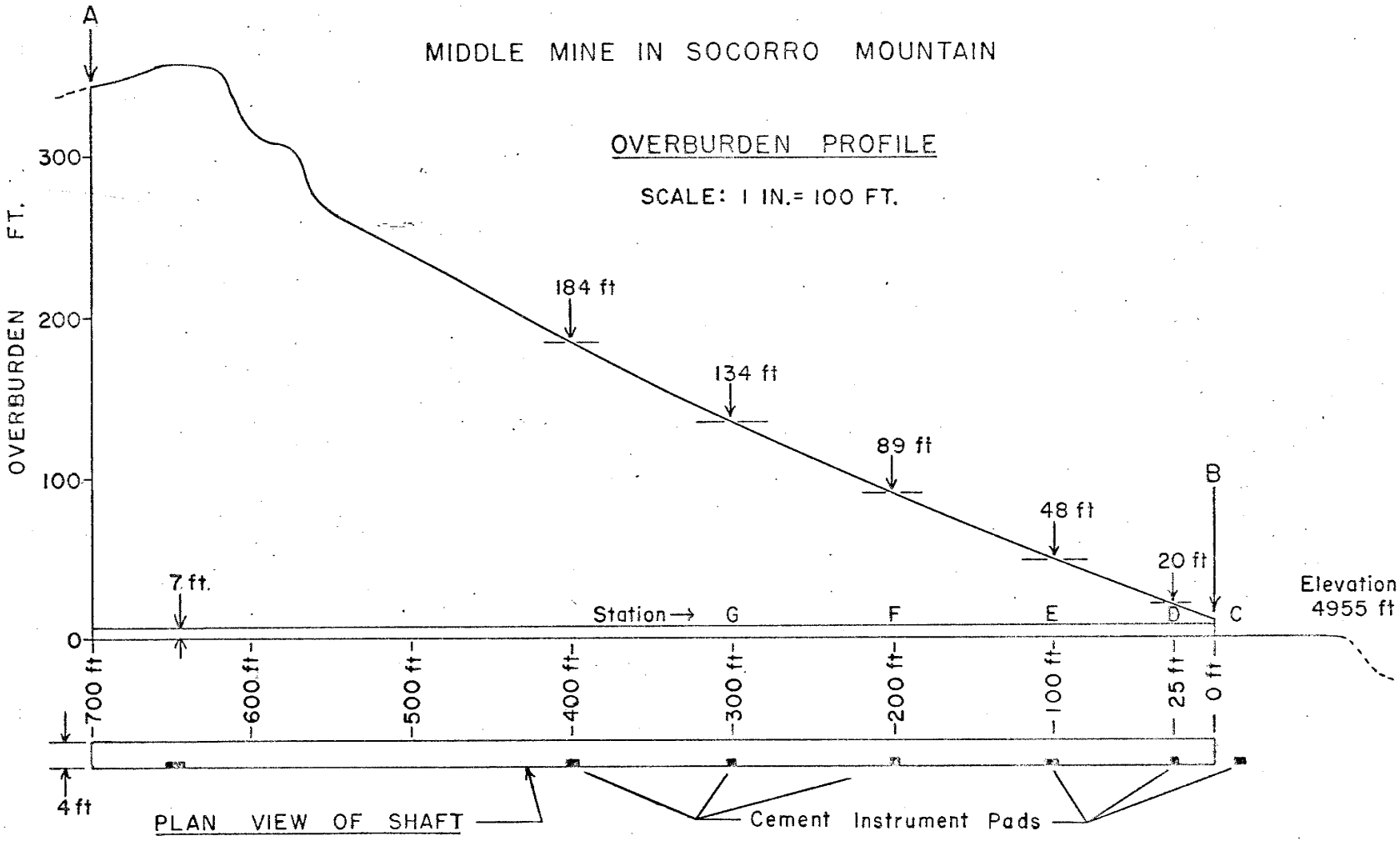

Figure 3. Cross-section of mine tunnel showing location of instrument pads.

INSTRUMENTS

The instruments used consisted of (1) four vertical transducers (Willmore seismometers) and (2) two recording units each containing amplifiers and pen and ink oscillographs for two input signals (Offner Dynagraph Recorder). Each transducer was wired directly to one of the four available input channels.

The Willmore seismometers were used as vertical ground-motion detectors. Mechanically they behave as displacement meters for frequencies greater than their natural frequency. The seismometer is a transducer which converts motion into an electrical signal and therefore the output is proportional to the ground velocity. The open circuit response of a Willmore is about 1 volt per unit ground velocity of 1 cm/sec. The natural frequency of the damped seismometers ranged from 1.3 cps with metal (iron) surrounding the instrument to 1.6 cps without the metal. Damping was controlled by a resistor in parallel with the transducer. Two values of resistance (270 ohms and 1000 ohms) were used in this study. The four seismometers showed a range of damping due to the presence of extra metal around two seismometers. About 70% of the events were recorded with damping between 0.31 and 0.45 of critical (270 ohms) and the remaining 30% were recorded with 0.16 to 0.28 of critical (1000 ohms). The high end of the range of damping was for instruments with extra metal shielding. The added metal surrounding the seismometer was to shield the transducers from 60 cycle

high-line pickup at two locations (stations C and D).

The short period instruments used in this study will not correctly register ground motions with frequencies below 2 or 3 cps when damped at less than 0.5 of critical. This immediately eliminates sources of data with periods of motion longer than 0.33 sec.

The amplifier-recording units were operated at sensitivities of 0.1mv/cm and 0.05 mv/cm (0.05×10^{-3} volts/cm) of pen displacement. Identical gains settings were used on all channels when recording. Frequency response of the recorder was good from DC to at least 50 cps. Recording was done on strip chart paper at 25 mm/sec. Calibration using internal signals in the recorders indicated response was within 5% on all channels. A test for pen fling showed less than 2% difference in trace amplitude for each recorder.

The magnification of the complete system, transducer plus recorder, is dependent on frequency. An input signal of 20 cps was magnified 8.8×10^5 times at a sensitivity of 0.05 mv/cm and with a damping resistance of 270 ohms.

Uniformity of trace amplitude on all channels was checked by using combinations of recorders and seismometers. The procedure was simplified because the seismometers were used in pairs while recording data and each pair of seismometers remained with one recorder. Each recorder and its transducer were checked for differences in trace amplitude by exchanging input leads from the instruments and producing spikes for each input arrangement. A cross-check between the

two channels on each recorder was made by comparing spikes on one channel of one recorder with each of the second recorder's channels. This cross-check is then repeated for the first recorder's second channel and again each of the channels on the second recorder. The results showed all trace amplitudes within 10% for average displacements of 8 to 12 mm. The error was under 5% for 75% of the cases and less than or equal to 2% for 40% of the cases. In general, the smaller errors were associated with displacements on the order of 3 to 6 mm (the order of magnitude of the larger first motions from microearthquakes recorded for this study).

DATA

SOURCES

Microearthquakes

Microearthquakes were the principle source of data for vertical ground motions because of their basic characteristics and high rate of occurrence (Sanford and Holmes, 1962). They represent a natural source (non-steady-state) of high-frequency elastic body waves. Figure 4 shows a microearthquake seismogram recorded on the free surface. The event begins at point A with the first P arrival and lasts for about 12 seconds. The S-P interval for this event was 1.7 seconds.

Microearthquakes in the Socorro region have epicentral distances ranging from 3 to 30 km and depths ranging from about 2 to 10 km. The majority are located within 16 km and are to the west and southwest of the stations used in this study. The average angle of incidence for microearthquakes at the tunnel location is 18 degrees (Personal communication, Sanford). Their magnitudes are negative on the Richter scale.

Frequencies for the first half-cycle of the P motion varied from 6 to 30 cps for events recorded during this study. Frequencies in the P phase portion of the seismogram (A to B in Figure 4) were in the neighborhood of 15 to 40 cps. The frequency of the first P motion of a microearthquake was always lower than frequencies in the seismogram immediately following the first full cycle. The frequency content of the maximum S motion in a seismogram (after B in Figure 4) was in

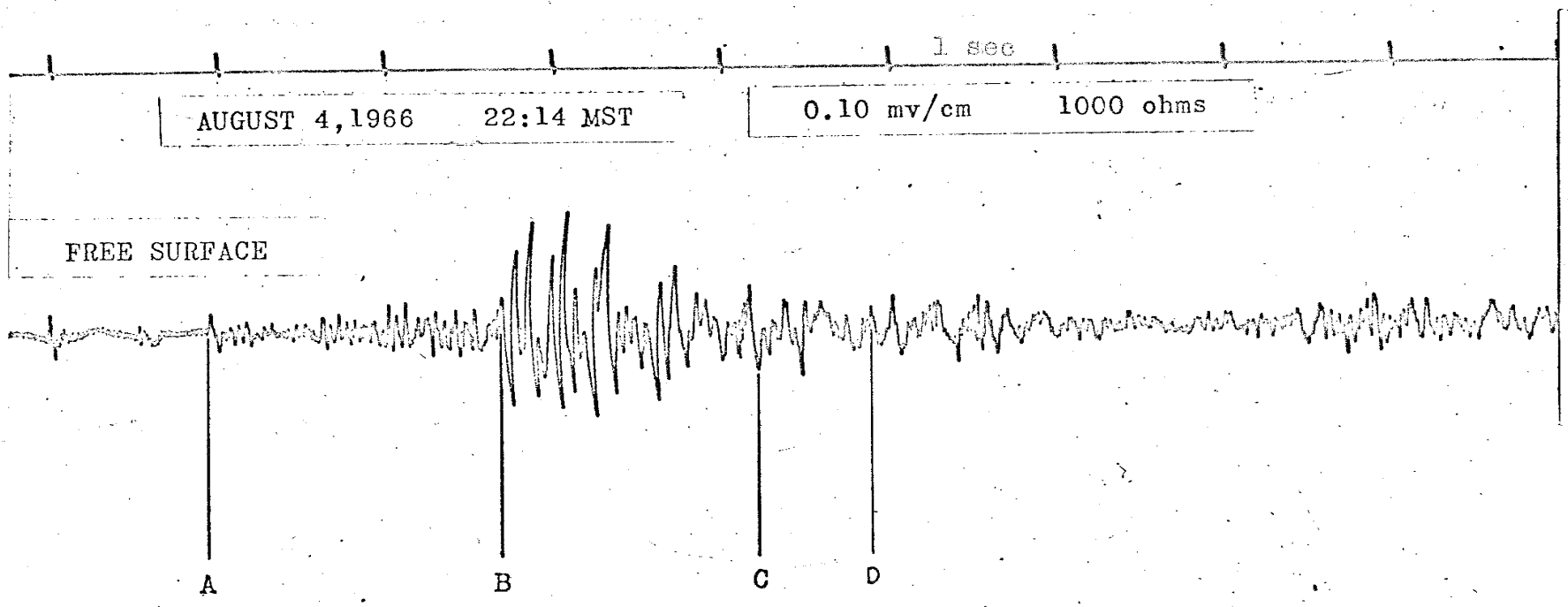

Figure 4. A microearthquake recorded at the free surface (Station C).

the range from 8 to 20 cps. The frequency of the first motion for microearthquakes was generally higher than the average frequency of the maximum S motion. This relationship is shown in Figure 5 as a plot of first motion frequencies versus S motion frequencies.

The frequency content of the seismogram in Figure 4 (ground motion on the free surface) is shown in Figure 6 by means of the power spectra of two different segments of the trace. The intervals between AB and BC were digitized using a time interval (Δt) of 0.01 seconds. The power spectra were then obtained by using a computer program based on the procedure of Blackman and Tukey (1958). The interval from A to B is believed to be primarily P phase arrivals and the interval from B to C is believed to be composed primarily of S phase arrivals. The frequency peak at 14 cps in Figure 6 is believed to be the dominant frequency of the S phase arrivals in the BC portion of the seismogram. The broad peak at frequencies from 17 to 20 cps (dashed line spectra) is thought to be the concentration of high frequencies in the P phase portion of the seismogram. There is also some indication of high frequency (21 cps) in the S phase portion of the seismogram. A frequency of 21 cps seems to be present in both segments of the seismogram.

The measured frequency of the first motion for the microearthquake in Figure 4 was 15 cps and the estimated dominant frequency of the maximum S arrivals was 13 to 14 cps. An estimate of the dominant frequency for interval AB in the

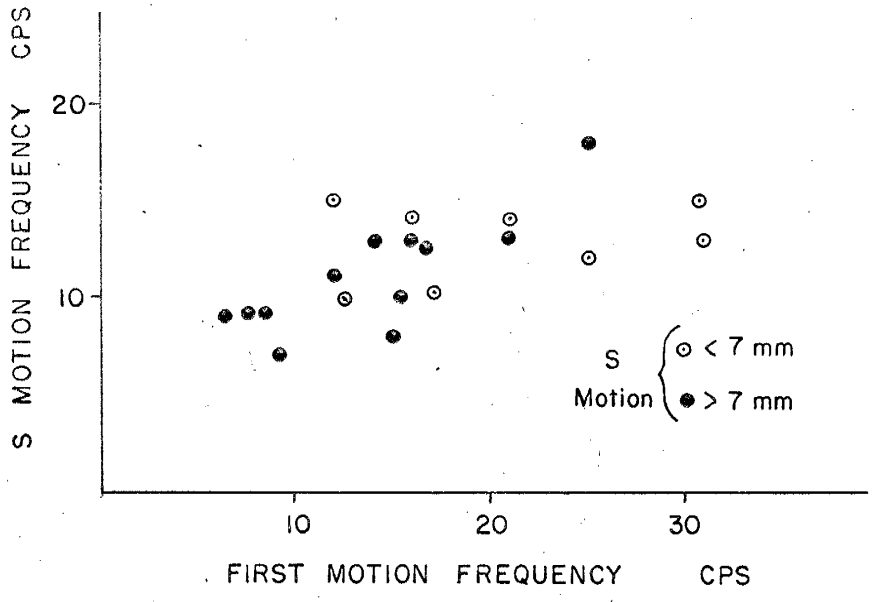

Figure 5. Plot of S motion frequency against first motion frequency.

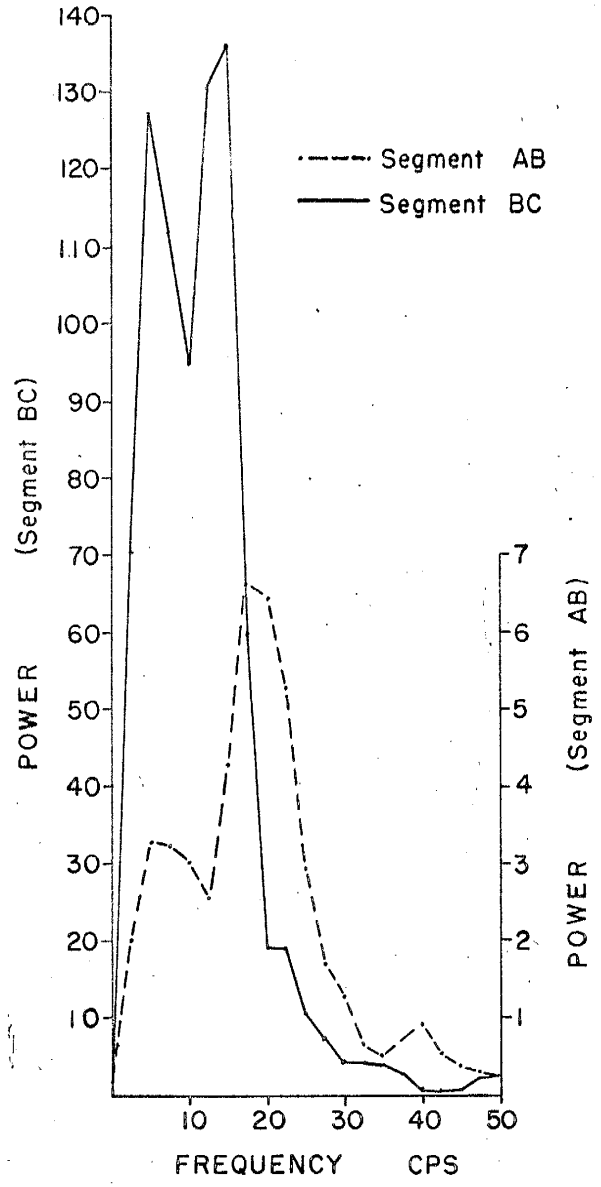

Figure 6. Power spectral density of the P and S arrivals of a microearthquake recorded at the free surface.

seismogram shown in Figure 4 was in the neighborhood of 20 cps. The agreement between power spectra frequency estimates and measured frequencies is good. This particular microearthquake has a frequency content which is typical of events of this strength.

Man-Made Seismic Events

Two sources of elastic waves produced by man were available for the study. Local unconfined surface explosions in a nearby canyon (Figure 2) produced a seismogram with measurable first motions having a frequency of 12.5 cps. The angle of incidence for these surface explosions is about 22 degrees (Personal communication, Sanford) and the distance is about 3 km. Mining explosions near Santa Rita, New Mexico produce longer period oscillations than the nearby explosions. First motions on the seismogram of a mining explosion were often weak and frequencies were usually too low (2 cps). Possible converted phases which follow the first motion of Santa Rita explosions have larger amplitudes and higher frequencies than the first motion.

ACQUIRING DATA

Microearthquake activity was primarily recorded from 2100 to 0600 hours to avoid microseisms of cultural origin. One recorder and two seismometers were operated intermittantly from June 10 to July 16, 1966. Fifteen usable microearthquakes were recorded on eleven nights. One seismometer was

placed at the free surface (station C) while the other was positioned first at the 200 foot pad (station F) and then moved at a later date to the 300 foot pad (station G). Two recorders and four seismometers were used from July 17 to August 26, 1966. Again one seismometer was at station C and the remaining three were placed on different pads inside the tunnel. Nineteen usable microearthquakes were recorded on twelve nights.

The nearby surface explosions were recorded between 0900 and 1600 hours. Data were taken in January and February with both seismometers inside the tunnel. One record was made in August with four seismometers including one at the free surface.

Mining explosions from Santa Rita were also recorded in January and February but only inside the tunnel. Two sets of usable traces were recorded with a four seismometer array, one each in July and August.

TREATMENT OF RECORDS

On the seismograms of each event the following measurements were made: (1) the amplitude of the first motion, (2) the frequency of the first half-cycle, (3) the amplitude of the maximum S motion, (4) the frequency of the maximum S motion, and (5) the S-P interval. First motion amplitudes were measured to the nearest tenth of a millimeter. The measured trace amplitude for first motions was the amplitude

of the first half cycle of P wave motion. S motion amplitudes were estimated to the nearest tenth of a millimeter but were considered accurate only within a half a millimeter. They were measured as the maximum width of an envelope drawn through the S motion peaks. Frequency of the first motion was calculated from the time for the first half cycle. Frequencies computed in this way were accurate to a half a cycle per second. Frequencies of the S motion were measured on the basis of averages for a number of cycles for one trace then repeated for other traces of the same event. Errors for these averaged frequencies were assumed to be plus or minus one cycle per second. The S-P interval was measured to the nearest tenth of a second.

PRESENTATION AND DISCUSSION OF DATA

AMPLITUDE AND FREQUENCY RELATIONSHIPS

The principle objectives in this thesis were to verify that the amplitudes of incident waves for real events (non-steady-state) are doubled at the free surface and to find the depth where the free surface effect does not influence the incident amplitude. Figure 7 shows two examples where amplitude doubling occurs in the first motions. Both events are microearthquakes of short duration with a small S-P interval (0.9 sec). The top trace in Figure 7A is ground motion at station C and the bottom trace is ground motion at station F. The first motion amplitude in the top trace is clearly twice the first motion in the bottom trace. The top trace in Figure 7B is ground motion at station C and the bottom trace is ground motion at station G. Figure 8 shows four traces at different stations for one event. This is also a microearthquake but the S-P interval is 1.7 seconds and the S phase motion is stronger than the events in Figure 7. The top trace is ground motion at station C and the remaining three traces are ground motion at stations D, E, and G. The first motion amplitude at station C is double the first motion amplitude at station G (bottom trace).

About fifteen microearthquakes indicated doubling in the first motion at the free surface with respect to the first ground motion at either station F or G. The majority of these microearthquakes were small events with first motion amplitudes near a millimeter. A number of events did not show a

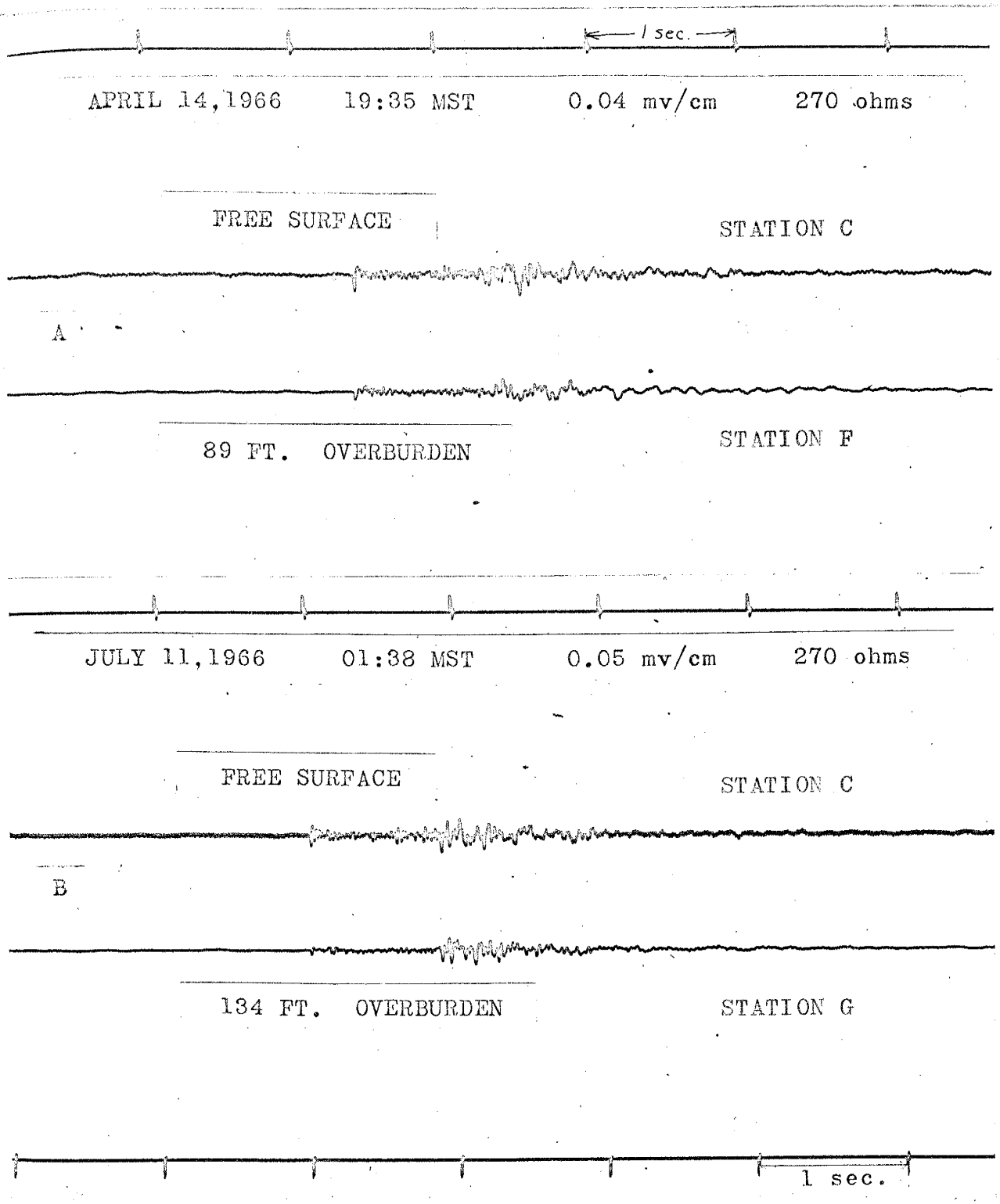

Figure 7. Two microearthquakes showing amplitude doubling in their first motions.

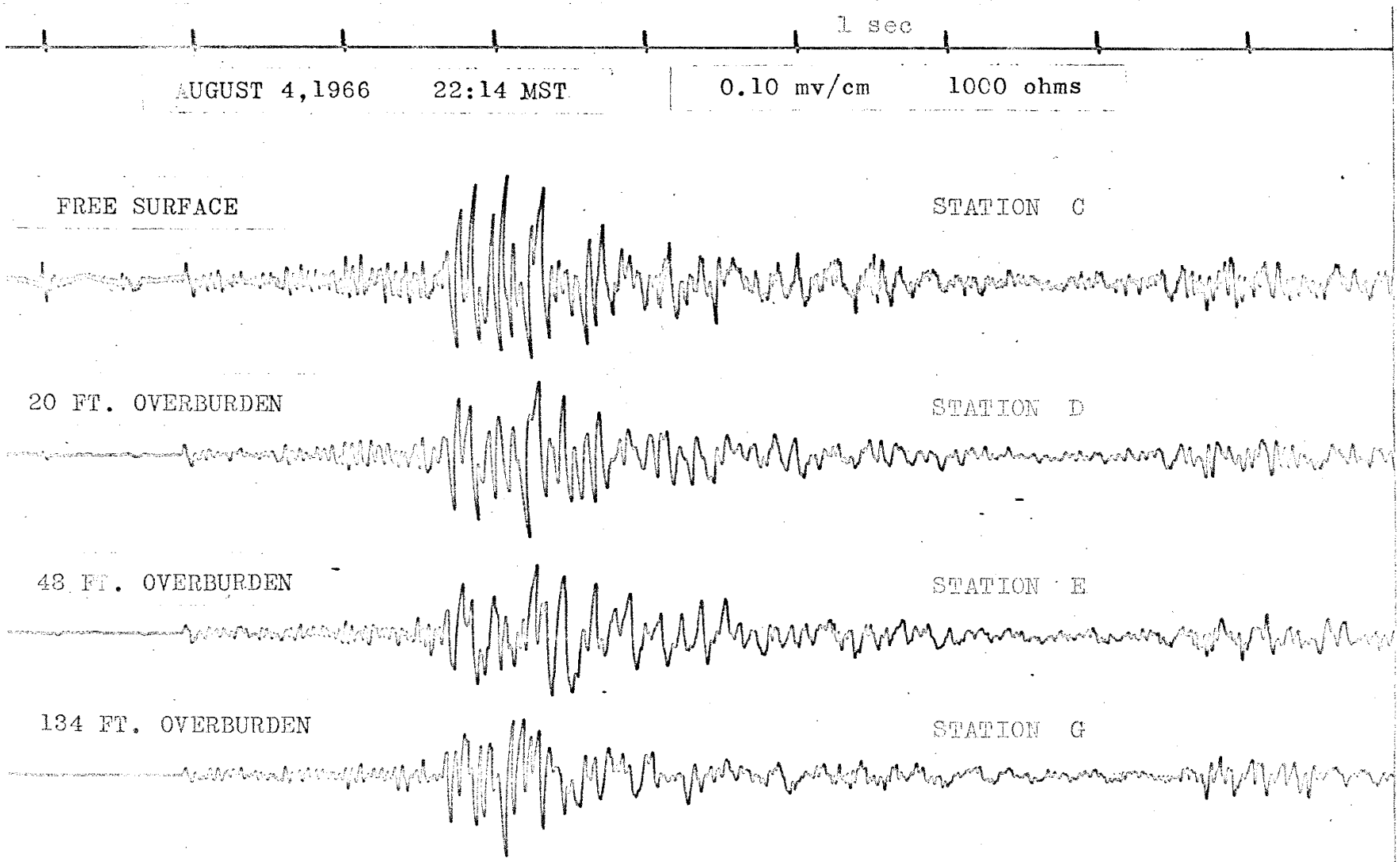

Figure 8. Four different traces of one microearthquake showing the effect of overburden thickness on trace amplitudes.

free surface doubling with respect to either station F or G. Most of these events had first motions with frequencies less than 15 cps. A few of the first motion amplitudes at the free surface, which were not doubled relative to either station F or G, had frequencies greater than 15 cps and abnormally large amplitudes.

The ratios of first motion amplitude at station C to first motion amplitude at either station F or G are plotted against the frequency of the first half cycle in Figures 9 and 10. These graphs show the effect of frequency on amplitude ratios. Each point in Figures 9 and 10 was weighted according to the trace amplitude of first motion at the free surface. An initial P motion greater than 2 mm was considered the most reliable and weighted with the largest circle. Figure 9 shows first motion amplitude ratios for ground motion at station C to ground motion at station F. At frequencies greater than 15 cps the ground motion at station C is double the ground motion at station F. Figure 10 shows first motion amplitude ratios for ground motion at station C to ground motion at station G. Amplitude doubling at the free surface relative to station G should exist for a wider range of frequencies. However, the data scatter is considerable and there are many points for first motion frequencies above 15 cps which indicate greater than expected displacements at station G. The points with amplitude ratios less than two at frequencies greater than 15 cps are from events characterized by a large first motion and a small S-P interval. At

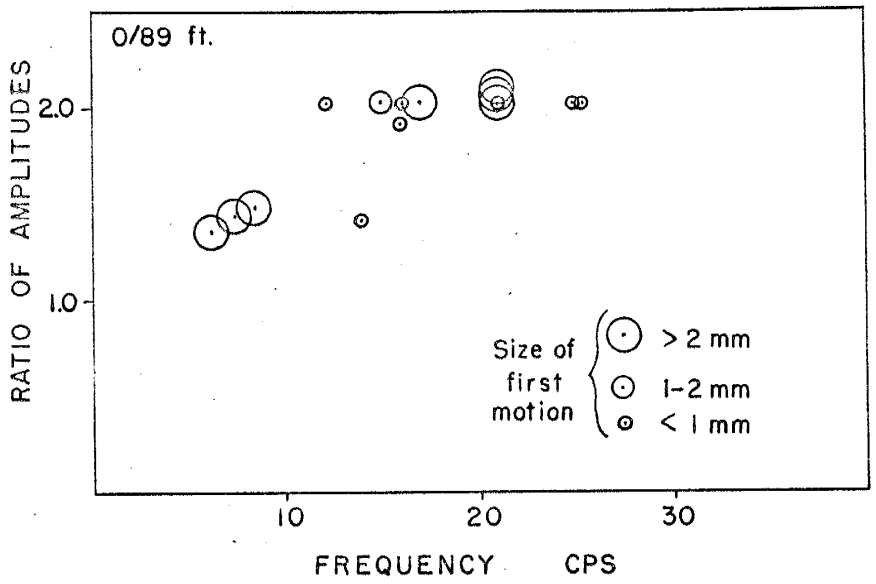

Figure 9. Ratio of amplitudes of first motions at station C to station F versus first motion frequency.

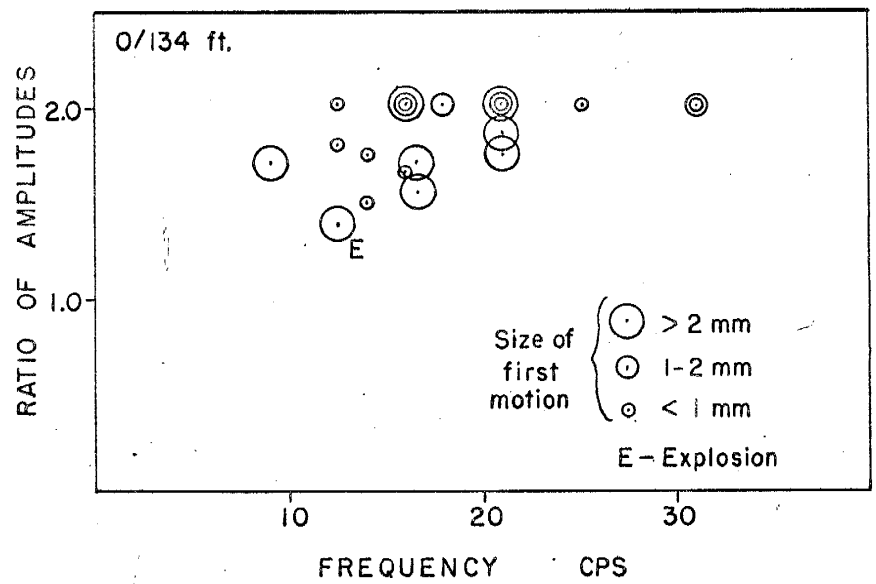

Figure 10. Ratio of amplitudes of first motions at station C to station G versus first motion frequency.

frequencies less than 15 cps in Figure 10 all but one point have amplitude ratios less than two. The event marked with the letter E is a local surface explosion.

First motion frequencies from 1 to 15 cps correspond to incident wavelengths from 10,000 to 666 feet assuming a rock velocity of 10,000 ft/sec. Figure 11 is a plot of amplitude ratios of ground motion at station C to ground motion at station F versus first motion wavelengths. At wavelengths less than 666 feet amplitude ratios are two. At wavelengths greater than 666 feet amplitude ratios for station C to station F are less than two and should approach one for very large wavelengths in the neighborhood of 10,000 feet. A wavelength of 10,000 feet is about 100 times the overburden depth at either station F or G. At this large a wavelength depths beneath the surface of 89 to 134 feet are not resolved and ground motion at these relatively shallow depths will also be doubled with respect to ground motion at very large depths.

Graphs similar to Figures 9 and 10 were plotted for amplitudes and frequencies of the S motion. Data for S arrival amplitudes at station F relative to S arrival amplitudes at station C are presented in Figure 12. The data shown in Figure 12 do not clearly indicate doubling. Scattering of points is extreme and may be due to errors in measurement of frequencies and/or peak to peak amplitudes of the S motion. Amplitudes of S motion at station G relative to S motion at station C were even more inconsistant than those in Figure 12

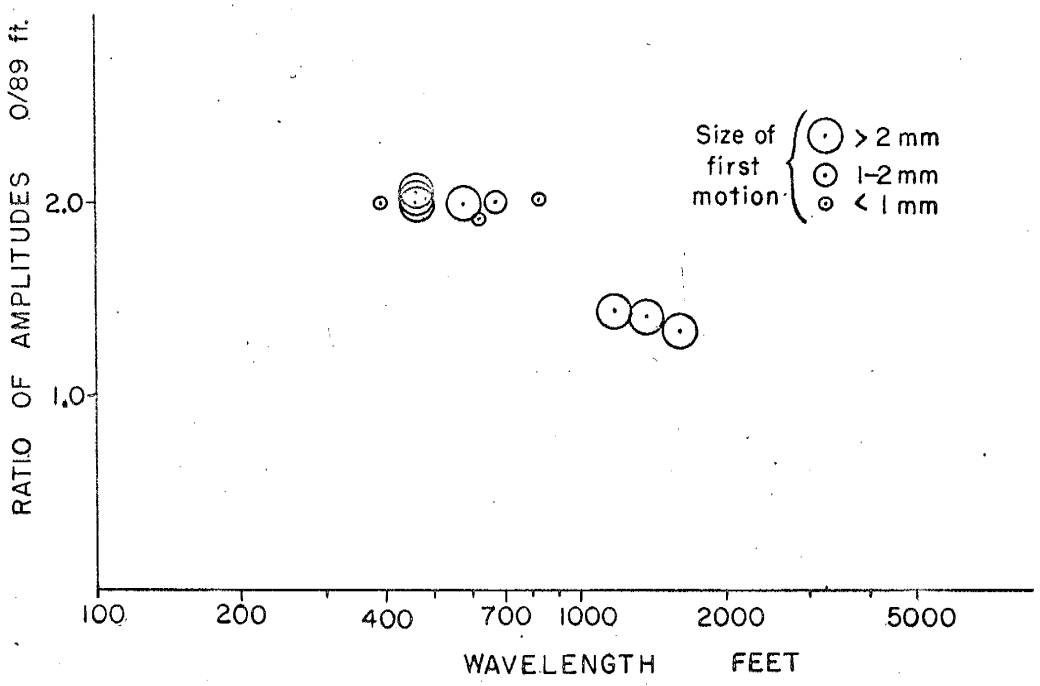

Figure 11. Ratio of amplitudes of first motions at station C to station F versus first motion wavelength.

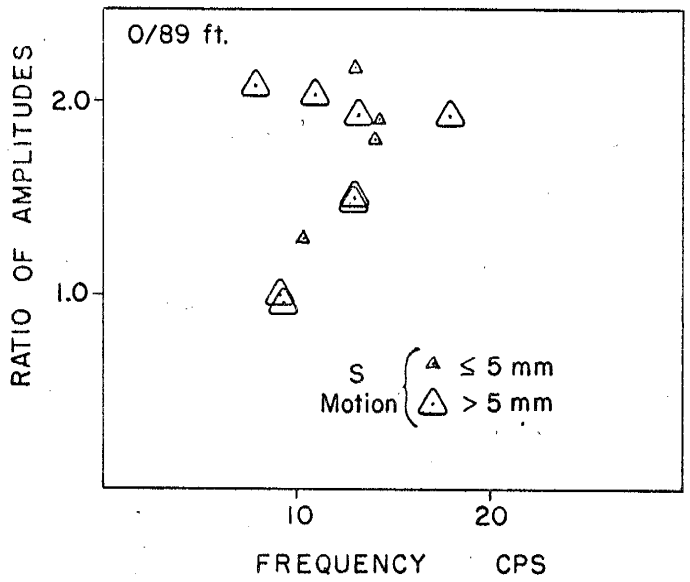

Figure 12. Ratio of amplitudes of S motions at station C to station F versus S motion frequency.

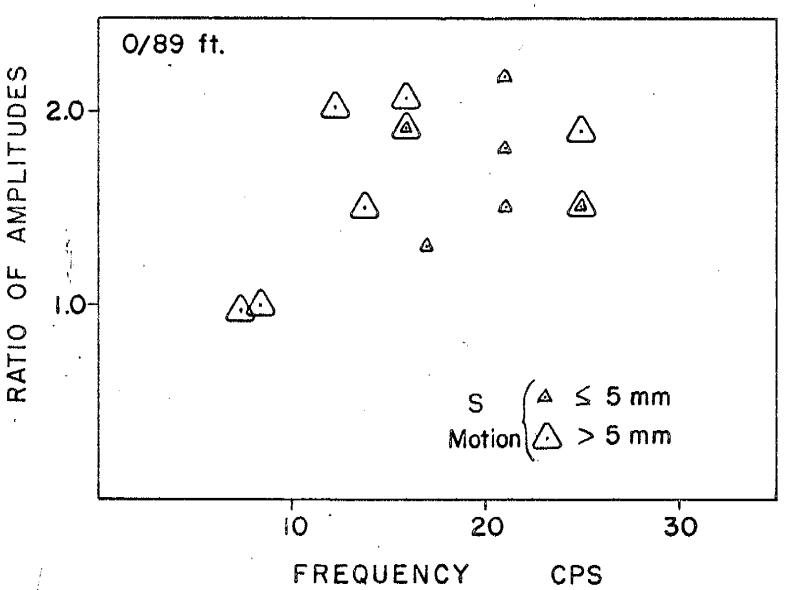

Figure 13. Ratio of amplitudes of S motions at station C to station F versus first P motion frequency.

despite a greater quantity of data.

Figure 12 was replotted using the frequency of the first P motion in place of the S motion frequency. The results given in Figure 13 are also scattered but there now appears to be a trend similar to Figure 10 that may indicate S motion amplitude ratios are a function of frequency.

The P motion frequency was used in Figure 13 because it is easier to measure and thus would be a more reliable parameter. Figure 5 shows that the measured P motion frequency is related to the measured S motion frequency in possibly a linear manner. This might also justify the use of the P motion frequency.

Theoretical vertical component S motion amplitudes at the free surface relative to S motion amplitudes far beneath the surface are greater by an average of 2.17 for incident angles less than 30 degrees. Figure 13 shows only three points where measured S motion amplitudes at station C were more than twice the S motion amplitudes at station F.

None of the observed S motion ratios for station C and station G were greater than two and only one had a value of two. The average amplitude ratio for these two stations was estimated to be about 1.6 for P motion frequencies from 9 to 25 cps.

AMPLITUDE AND OVERBURDEN RELATIONSHIPS

Figures 14, 15, and 16 are graphs of first motion amplitudes (for different intervals of frequency) versus overburden thickness. The ground motion amplitudes for each event were normalized to a free surface amplitude of one, and thus amplitudes below the surface range from 0.5 to 1.0. As before, points in each graph were weighted according to the amplitude of the first motion at the free surface.

Figures 14 and 15 are for first motions with frequencies in the ranges 21-31 cps and 15-20 cps. Both graphs are very similar in character. The maximum reduction in amplitude (0.5) appears to occur at a depth of less than 50 feet for both frequency ranges. The largest incident wavelength in these frequency ranges is 666 feet or about thirteen times the minimum depth required for maximum amplitude reduction. Therefore the maximum amplitude change is occurring at small depths compared to the wavelengths.

Figure 16 is a plot of first motions in the frequency range of 6-9 cps. The maximum amplitude reduction appears to occur at a depth greater than 134 feet.

Since trace amplitudes on the seismograms are a measure of particle velocities the former are proportional to the frequency of ground motion. Figures 14 through 16 present data for ranges of first motion frequency. Some of the spread in data points may be a result of the range of frequencies of first motion considered in each graph.

S phase amplitudes as a function of depth beneath the

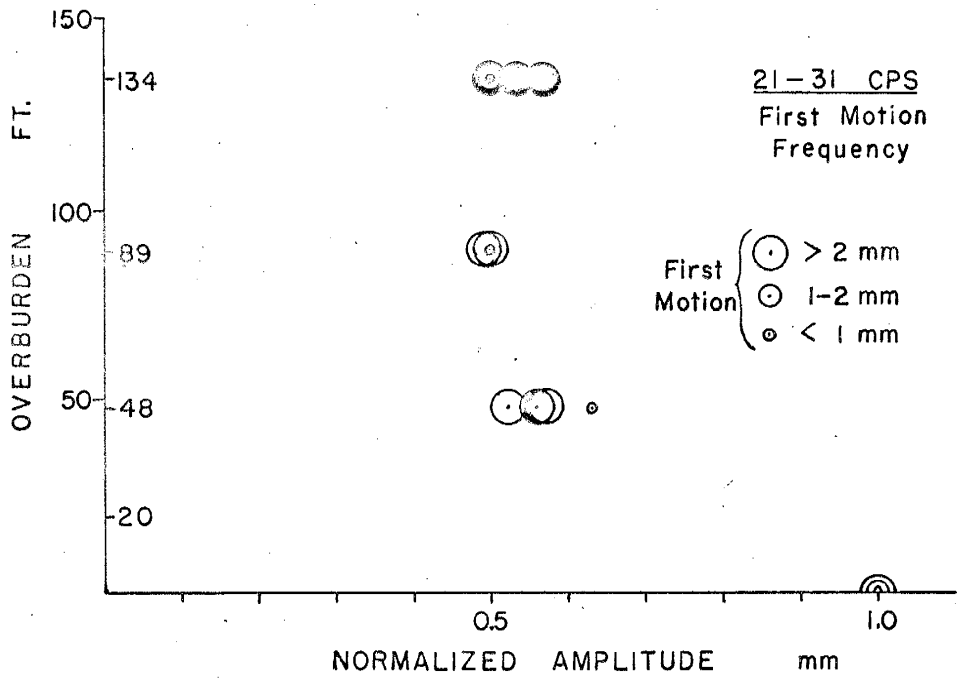

Figure 14. Relative first P motion amplitudes versus overburden for frequencies from 21 to 31 cps.

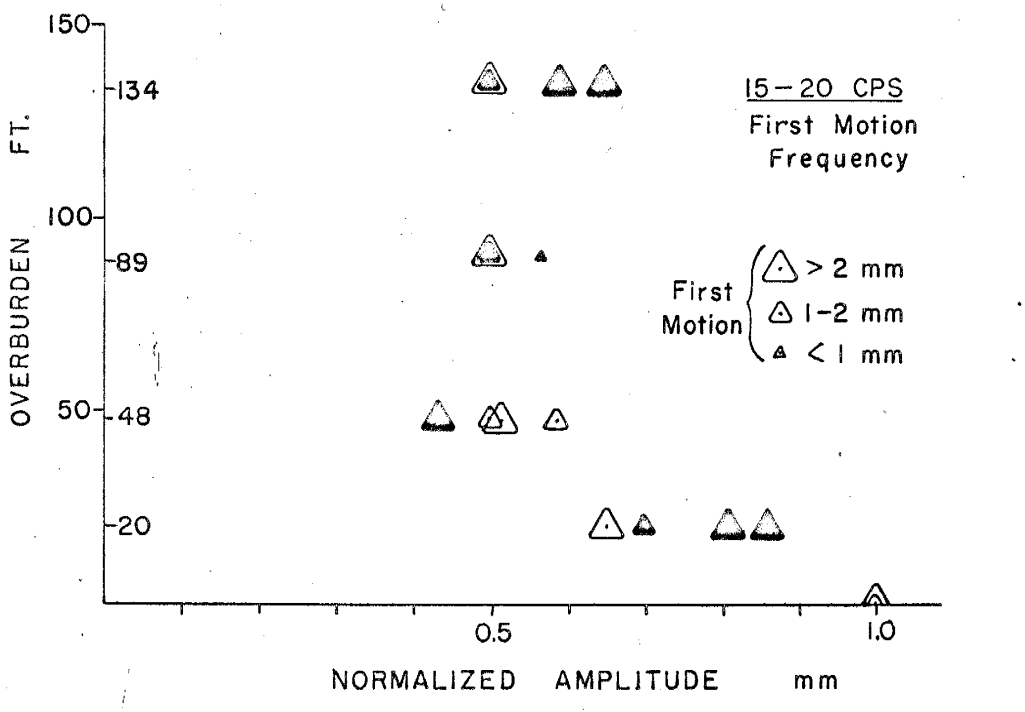

Figure 15. Relative first P motion amplitudes versus overburden for frequencies from 15 to 20 cps.

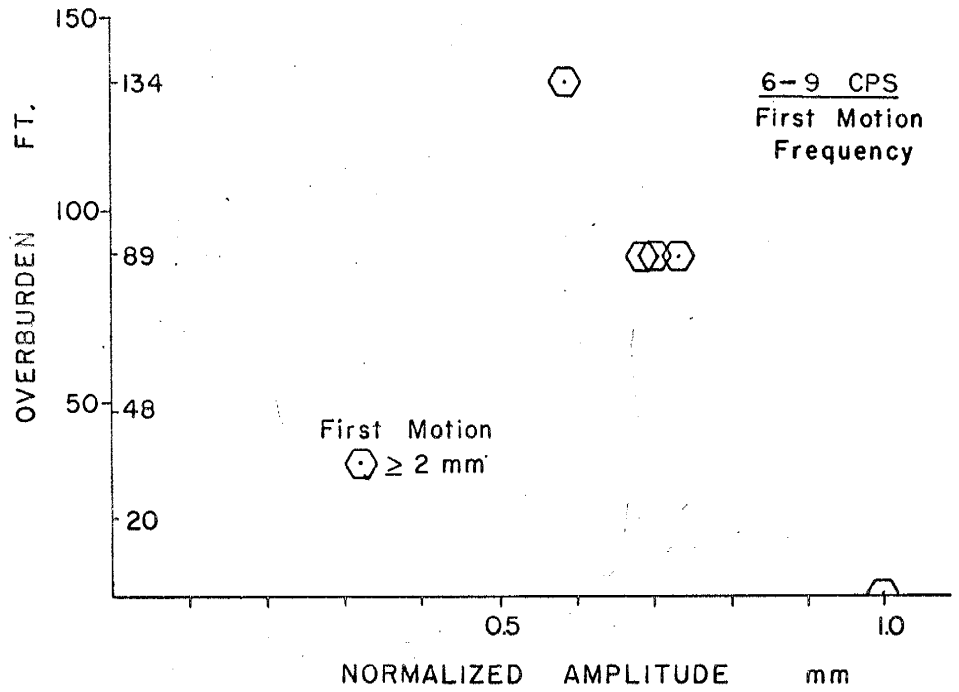

Figure 16. Relative first P motion amplitudes versus overburden for frequencies from 6 to 9 cps.

surface are given for two ranges of S motion frequency in Figures 17 and 18. The decrease in amplitude with increase in depth beneath the surface is more gradual in the case of S motion than in the case of P motion. Theoretically the maximum expected S motion amplitude reduction at depths far beneath the surface should be 0.46 with reference to the free surface amplitude. It does not appear that any of the stations are sufficiently deep for the maximum reduction in amplitude. This may be due to the presence of low frequency in the S phase. The power spectra in Figure 6 for the S arrival portion of the microearthquake in Figure 4 shows a strong peak at a frequency of 5 cps. An S wave with a frequency of 5 cps may not change in amplitude in the depth range used in this study. A visual examination of the microearthquake in Figure 8 does suggest that the low frequency oscillations in the S phase are unaffected by increase in depth beneath the surface while the higher frequency oscillations definitely decrease. The exception to this generalization appears to be the S motion recorded at station G.

Examples of additional seismograms recorded for this study are shown in Figures 19, 20, and 21. Figure 19 shows traces of a microearthquake very similar in character to the event in Figure 8 but with a slightly lower first motion frequency (12 cps). The first P motion amplitude at either station F or G is half the corresponding amplitude at station C. This event had the lowest first motion frequency (12 cps) for amplitudes at station F or G which still showed the

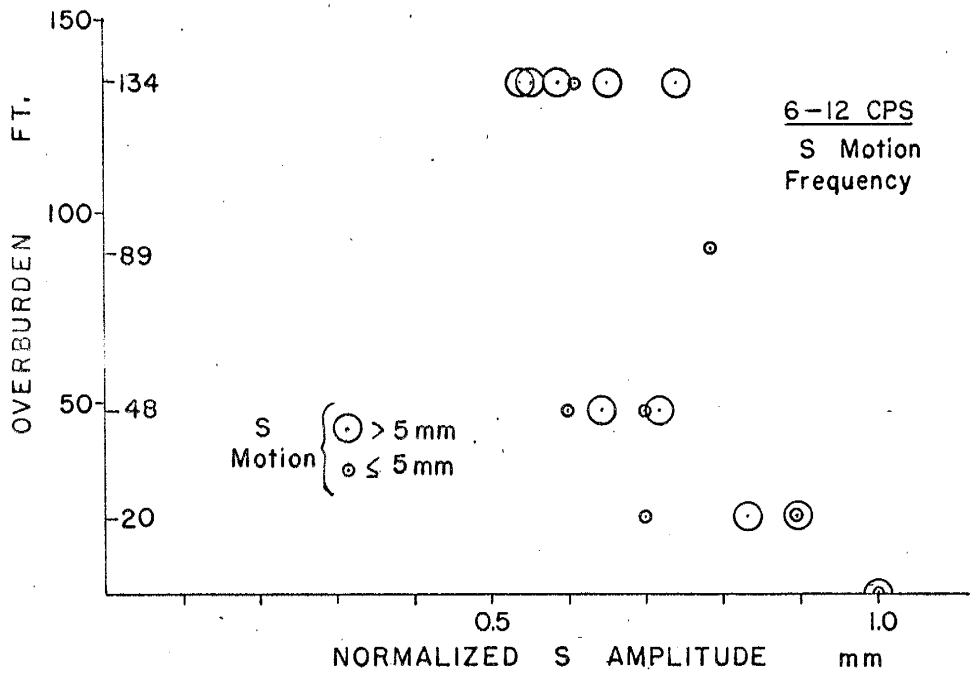

Figure 17. Relative S motion amplitudes versus overburden for S motion frequencies from 6 to 12 cps.

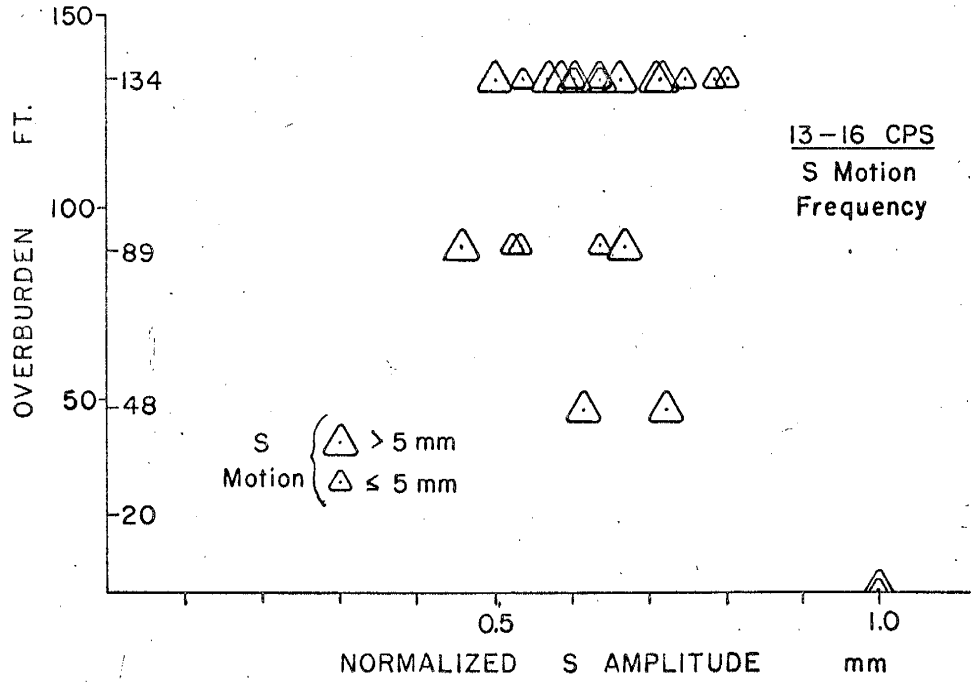

Figure 18. Relative S motion amplitudes versus overburden for S motion frequencies from 13 to 16 cps.

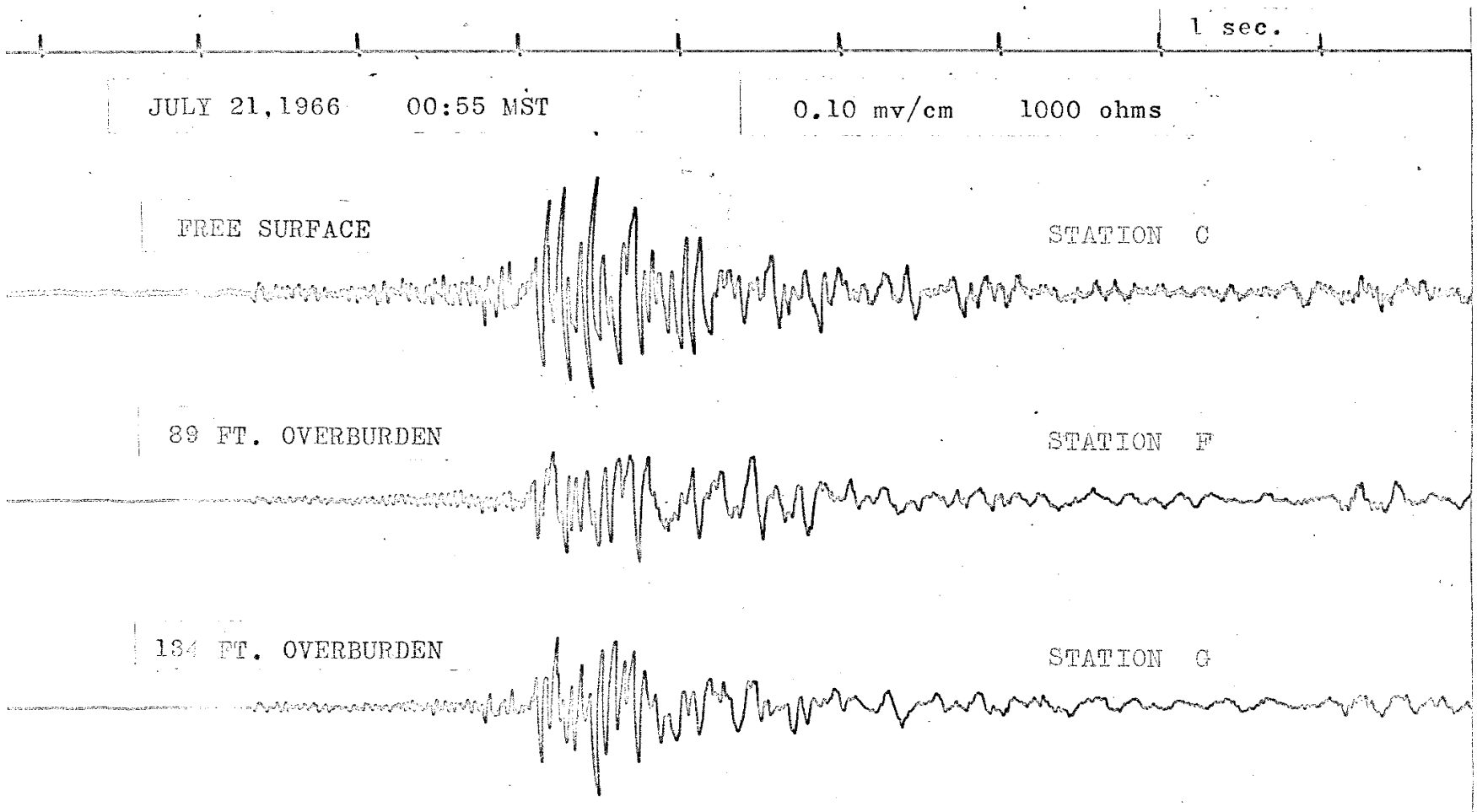

Figure 19. Three traces of one microearthquake showing S phase amplitude increase at station G relative to station F.

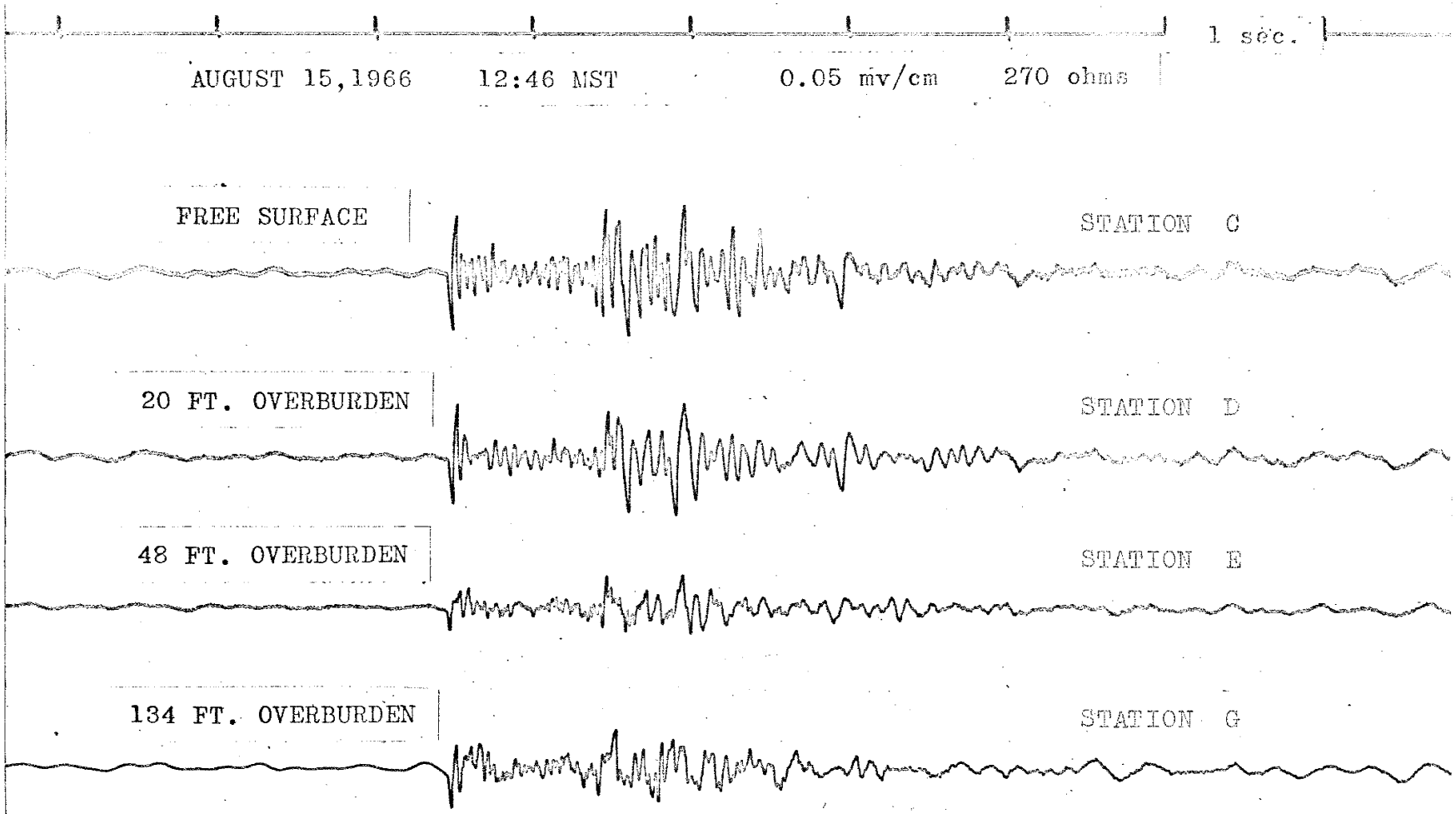

Figure 20. Four different traces of one microearthquake showing the effect of overburden thickness on amplitude.

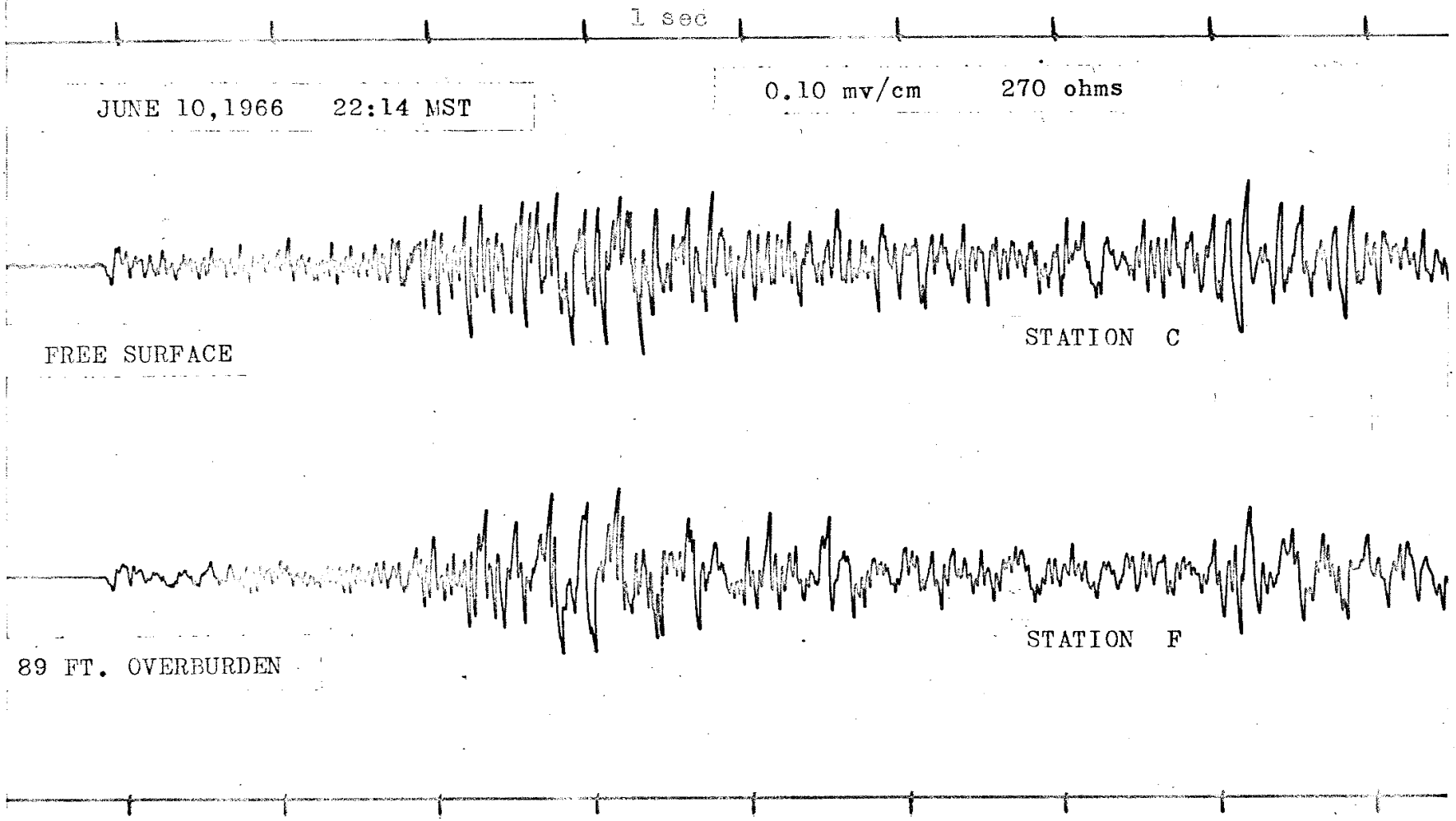

Figure 21. Two traces of a microearthquake showing the effect of low frequency on the amplitude of the first motions.

maximum amplitude reduction (0.5). This figure shows an increase in amplitude of the S phase at station G when compared to the amplitude at station F. A number of events had similar S phase amplitude changes at station G. This may indicate reinforcement between reflected waves from the surface and the incident waves.

The first motion amplitudes in Figure 20 are anomalous. The first motion amplitude recorded at station G is larger than the amplitude at station E. This event is characterized by a short S-P interval (1.0 sec) and a large first motion amplitude relative to the S motion amplitude. Other events with a short S-P interval and a large first motion amplitude relative to the S motion amplitude were the only sources of the anomalous amplitude increases at station G. The first motion amplitude at station E is abnormally small when compared to station C. In addition, the motion following the first half cycle is unlike the other three traces. A recording of a smaller event identical in all respects except amplitude to the one shown in Figure 20 also showed the same small first motion at station E. The reasons for anomalous amplitudes of the first motion at the underground stations is unknown. Points in Figures 14 and 15 which are taken from records with characteristics similar to Figure 20, are blacked in for identification purposes.

Figure 21 is a microearthquake recorded at stations C and F. The first motion amplitude was not halved at a depth of 89 feet because this depth was not great enough to isolate

the relatively low frequency first motion (8 cps) from the effect of the free surface. The S phase amplitude at station C is about the same as the S phase amplitude at station F. Again the presence of the low frequency in the S motion is assumed to be responsible for the lack of change in amplitude at station F relative to station C.

FREQUENCY FILTERING

A visual examination of the microearthquake seismograms in Figures 8, 19, 20, and 21 indicate the high frequency content of the seismogram is to some extent dependent on the seismometer location. High frequencies appearing on the trace for station C (free surface) are usually absent on the traces for stations D, E, and F. However, at station G these same high frequencies seem to remain in the seismogram.

The traces recorded at stations C, E, and G in Figure 8 were digitized over the same interval of time (the interval A to D in Figure 4) and power spectra computed (Figures 22, 23, and 24, respectively). The high frequencies (14 and 21 cps) at station C (Figure 22) are missing at station E (Figure 23), but are present at station G (Figure 24). It is not known why there are high frequency peaks in Figure 24 and not in Figure 23 since each represents the frequency content of a seismogram recorded in a similar environment but at a different location. The addition of a low frequency peak at 2 cps is suggested in Figure 23 and is quite prominent in Figure 24

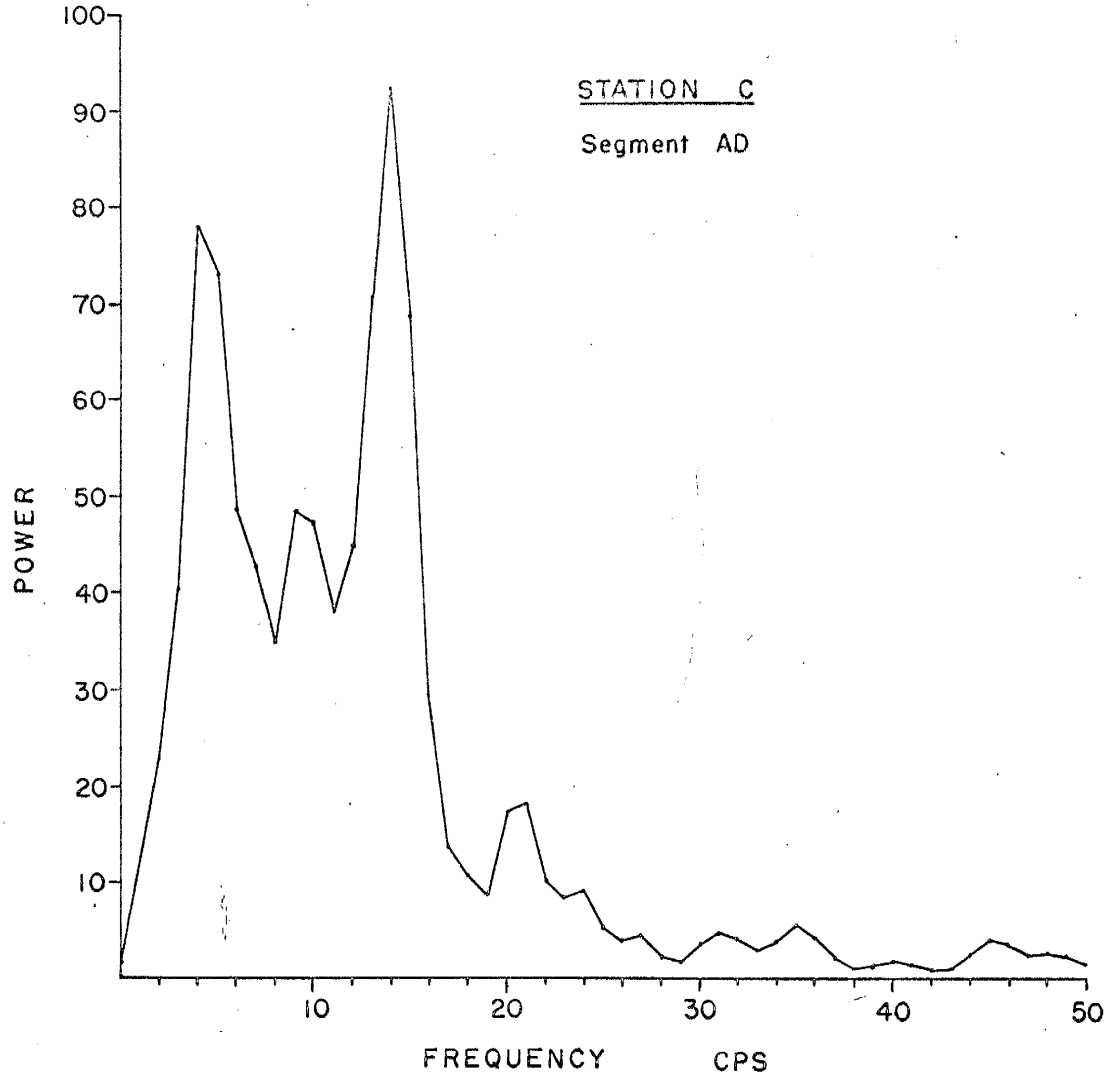

Figure 22. Power spectrum of a microearthquake trace (August 4, 1966) at station C (free surface).

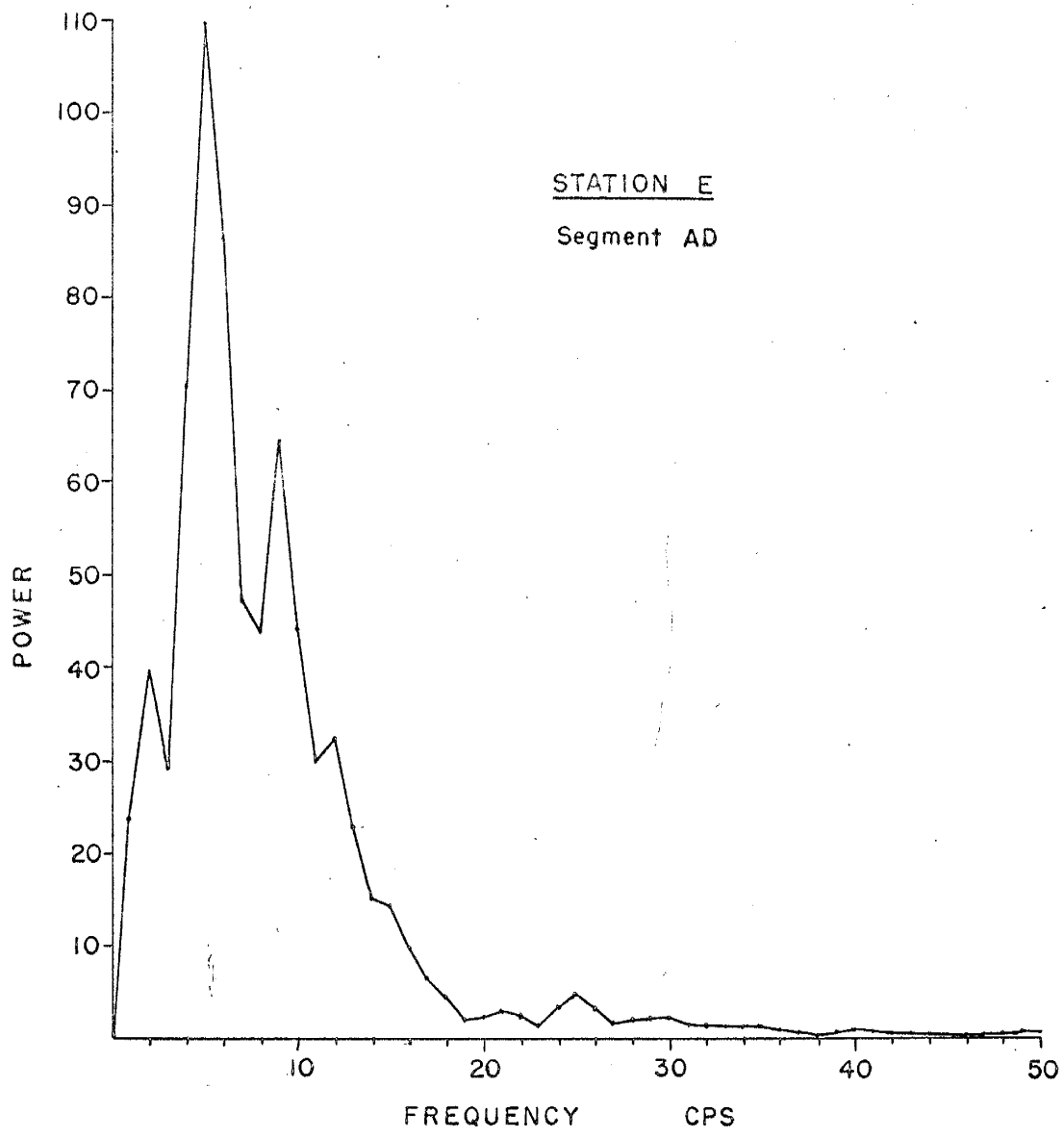

Figure 23. Power spectrum of a microearthquake trace (August 4, 1966) at station E (48 feet overburden).

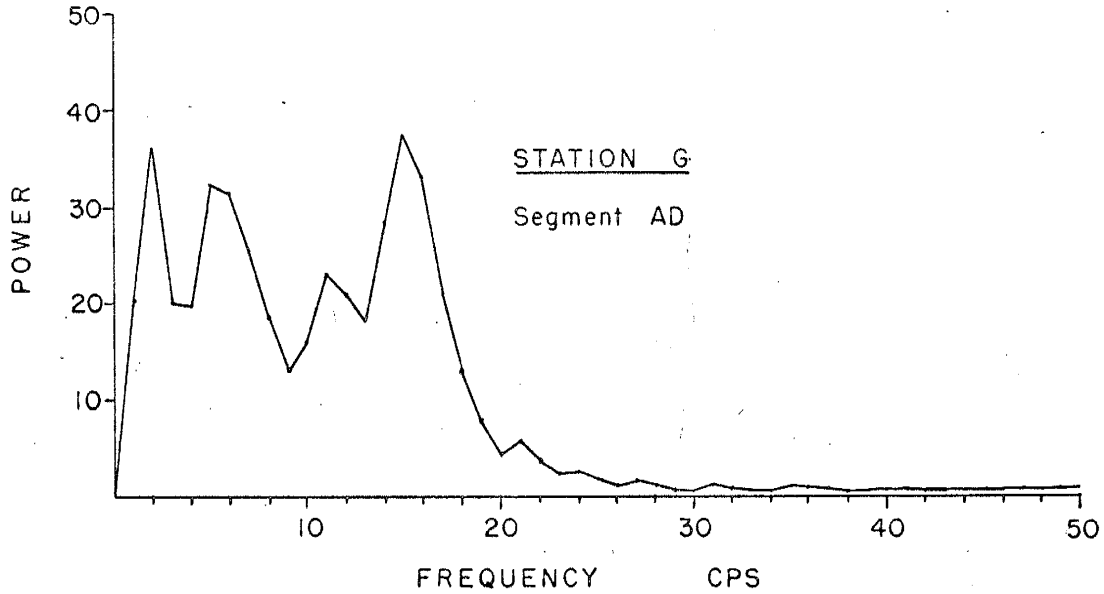

Figure 24. Power spectrum of a microearthquake trace (August 4, 1966) at station G (134 feet overburden).

although the total power in the peak remains about the same as in Figure 23.

CONCLUSIONS

The amplitudes of initial P motion and S motion on microearthquake seismograms of a single event recorded at different depths show that ground motion at the surface is larger than ground motion beneath the surface. A non-steady-state source of elastic waves such as a microearthquake can be used to verify differences in ground motion which are predicted by assuming a steady-state source. Ground motion doubling at the free surface with respect to incident ground motion at depths of 89 and 134 feet beneath the surface was verified using amplitudes of first P motion arrivals.

The frequencies of first motion arrivals influenced the amplitude of ground motion at different depths. The maximum amplitude change for first motions with frequencies greater than 15 cps occurred in the first 50 feet below the surface. For first motion frequencies greater than 15 cps, amplitudes at the free surface were generally twice the measured incident amplitudes below 50 feet. First motion amplitudes with frequencies less than 15 cps at either station F or G usually did not show the maximum amplitude reduction (half the free surface amplitude) relative to amplitudes at station C (free surface).

S phase amplitudes as a function of frequency and depth were not well defined. Changes in S phase amplitudes as a function of the detector's depth for a range of frequencies was similar to the first motion amplitude changes

but were more gradual in the first 50 feet. S motion amplitudes at the free surface are theoretically an average of 2.17 times the incident S amplitudes (for angles of incidence less than 30 degrees). The maximum amplitude reduction of the free surface amplitude for S motions is therefore 0.46. With one exception the data did not show this large an amplitude reduction at either station F or G (overburden 89 or 134 feet). It is believed that the presence of low frequencies (4 to 5 cps) in the S phase were responsible for the large amplitudes at depths of 89 and 134 feet.

There were anomalous differences in trace amplitudes which cannot be explained. The S phase amplitudes occasionally showed an increase at station G when compared to station E and is thought to be either a reinforcement of incident waves and reflected waves from the surface or possibly the result of a velocity or density anomaly in the vicinity of station G. One particular set of events characterized by a short S-P interval and a strong first motion had larger first motion amplitudes at station G (134 feet overburden) than at station E (48 feet overburden). The location of these events may help to explain why these first motion amplitudes are different.

The high frequency content of the seismogram seems to be somewhat dependent on the seismometer's location. High frequencies in the free surface seismogram were generally absent in the seismograms at stations D, E, and F (overburdens of 20, 48, and 89 feet) but not in the seismograms at station

G (overburden 134 feet).

Future studies on ground motion at the same experimental site should establish new stations at greater depths and add instrumentation to measure direction and angle of approach. Data should be taken in a way that will allow the easiest digitalization for purposes of analyzing the records. A detailed velocity profile is needed along the tunnel.

REFERENCES

Blackman, R., and J. Tukey (1958), The Measurement of Power Spectra, Dover Publications, Inc., New York, 189 p.

Dix, C.H. (1952), Seismic Prospecting for Oil, Harper and Brothers, New York, p 214.

Ewing, W.M., W.S. Jardetzky, and F. Press (1957), Elastic Waves in Layered Media, McGraw-Hill Book Co., Inc., New York, 380 p.

Gutenberg, B. (1944), Energy ratio of reflected and refracted seismic waves, Bull. Seism. Soc. Amer., v.34, pp 85-104.

Kanai, K., and T. Tanaka (1951), Observations of the earthquake-motion at the different depths of the earth. I., Bull. Earthquake Research Inst., Tokyo Univ., v.29, pp 107-116.

Kanai, K., T. Tanaka, and S. Yoshizawa (1959), Comparative studies of earthquake motions on the ground and underground, Bull. Earthquake Research Inst., Tokyo Univ., v.37, pp 53-87.

Knopoff L., R.W. Fredricks, A.F. Gangi, and L.D. Porter (1957), Surface amplitudes of reflected body waves, Geophysics, v.22, pp 842-847.

Macelwane, J.B. and F.W. Sohon (1932), Introduction to Theoretical Seismology, Part I, St. Louis University, St. Louis, Missouri, p 166.

Richter, C.F. (1958), Elementary Seismology, W.H. Freeman and Company, San Francisco, Calif., p 670.

Sanford, A.R. (1962), Microearthquakes near Socorro, New Mexico, Jour. Geophys. Res., v.67, pp 4449-4459.

Shima, E. (1962), Modifications of seismic waves in superficial soil layers as verified by comparative observations on and beneath the surface, Bull. Earthquake Research Inst., Tokyo Univ., v.40, pp 187-259.

Smith, C.T. (1963), Preliminary notes of the geology of part of the Socorro Mountains, Socorro County, New Mexico, Guidebook New Mexico Geol. Soc., Socorro Region, 14th Field Conf.: 185-196.

This thesis is accepted on behalf of the faculty of the Institute by the following committee:

C E Jacob

Allan R. Sanford

Charles B. Holmes

W. J. Budelig

Date: 25 October 1966